

Supporting information

Efficient and stable photocatalytic H₂ evolution by Self-assembly of Zirconium(IV) coordination with perylene diimide supramolecule under visible light irradiation

Haoran Ding^{#a}, Zhiqiang Wang^{#b}, Kangyi Kong^a, Shufan Feng^a, Lifeng Xu^a, Haonan Ye^a,
Wenjun Wu^{*a} Xueqing Gong^{*b} and Jianli Hua^{*a}

^a Key Laboratory for Advanced Materials , Institute of Fine Chemicals, Feringa Nobel Prize Scientist Joint Research Center, School of Chemistry and Molecular Engineering, East China University of Science and Technology, 130 Meilong Road, Shanghai 200237, PR China

^bKey Laboratory for Advanced Materials and Joint International Research Laboratory for Precision Chemistry and Molecular Engineering, Feringa Nobel Prize Scientist Joint Research Center, Centre for Computational Chemistry and Research Institute of Industrial Catalysis, School of Chemistry and Molecular Engineering, East China University of Science and Technology, 130 Meilong Road, Shanghai 200237, PR China.

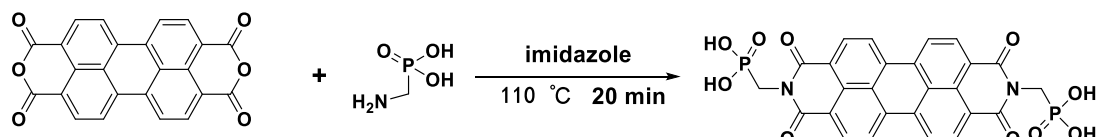
* Corresponding author. Tel.: +86 21 64250940; fax.: +86 21 64252758.

E-mail address: jlhua@ecust.edu.cn (J. Hua); xgong@ecust.edu.cn (X. Gong);
wjwu@ecust.edu.cn (W. Wu)

Table of Contents

Supporting information	S1
A self-assembled perylene diimide nanobelt for efficient visible-light-driven photocatalytic H ₂ evolution	
1. Preparation of P-PMPDI supramolecule	S1
2. Atomic force micrograph (AFM) of supramolecular	S2
3. Stability of supramolecular catalyst.....	S2
4. DRS and UPS spectroscopy of supramolecular P-PMPDI-Zr	S3
5. Light-harvesting ability and crystallinity of P-PMPDI-M	S4
6. Fourier transform infrared spectra of supramolecular	S4
7. Density functional theory (DFT) calculations	S5
8. Calculated apparent quantum yield (AQY) at different wavelengths	S6
9. The reported work previously	S7
10. References	S8

1. Preparation of P-PMPDI supramolecule



Scheme.S1 Schematic illustration of synthesis of **PDI** molecule

The synthesis of the **N, N'-bis(phosphonomethyl)-3,4,9,10-perylenediimide (PMPDI)** has been carried out by following previous work.^{1,2} Firstly, 790 mg (2.01 mM) 3,4,9,10-Perylenetetracarboxylic dianhydride, 470 mg (2.01 mM) (Aminomethyl)phosphonic acid and 15 g imidazole were heated at 130 °C for 40 minutes in a three-necked flask. Next 25 mL of 2M HCl and 25mL ethanol were mixed with ultrasound and added into the reaction mixture all at once. Solid precipitates would appear immediately and keep these suspensions stirring for another 30 minutes, and then dark solids were collected by centrifugation from above resulting mixture. Repeated deionized water washing and vacuum drying at 50 °C to obtain pure **PMPDI**. ¹H NMR (400 MHz, disodium salt, Deuterium Oxide) δ (ppm): 8.44 – 7.70 (broad, 8H), 4.41 – 4.10 (broad, 4H) (peak broadening was observed as a result of dye aggregation).³

Preparation of supramolecular **P-PMPDI**. First, above crude product (**PMPDI**) was dispersed in 300 mL deionized water, and it would dissolve in water by dropping 1M NaOH solution into mixture, and then filtrate was collected by centrifugation. After that precipitating the filtrate by adding 2M HCl solution until pH=1 thus supramolecular **P-PMPDI** formed, and finally collecting the dark solid by centrifugation to separate it from imidazole dissolved in the acidic solution. The collected solid was dried in oven at 50 °C overnight for further application.

2. Atomic force micrograph (AFM) of supramolecular

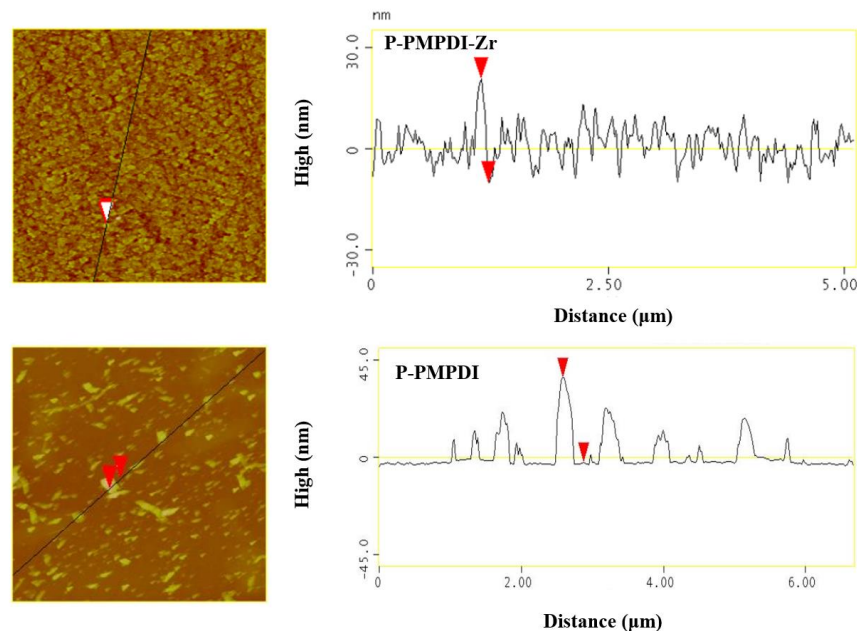


Fig S1. Atomic force micrograph (AFM) of **P-PMPDI-Zr (1:0.25)** and **P-PMPDI**.

3. Stability of supramolecular catalyst

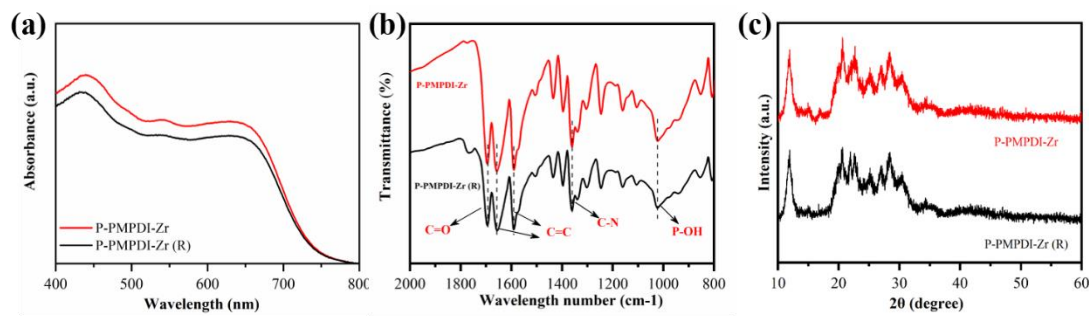


Fig. S2 (a) UV-vis DRS, (b)FT-IR and (c) XRD of **P-PMPDI-Zr (1:0.25)** and recovered catalyst **P-PMPDI-Zr (R)**

4. DRS and UPS spectroscopy of supramolecular P-PMPDI-Zr

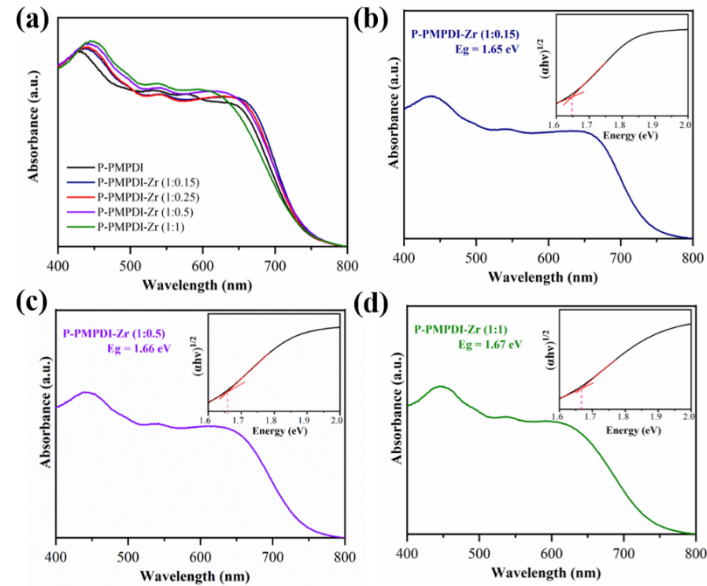


Fig. S3 UV-vis diffuse reflectance spectra of P-PMPDI-Zr (1:0.15), P-PMPDI-Zr (1:0.5) and P-PMPDI-Zr (1:1). Inset: the corresponding colors and the Tauc plots

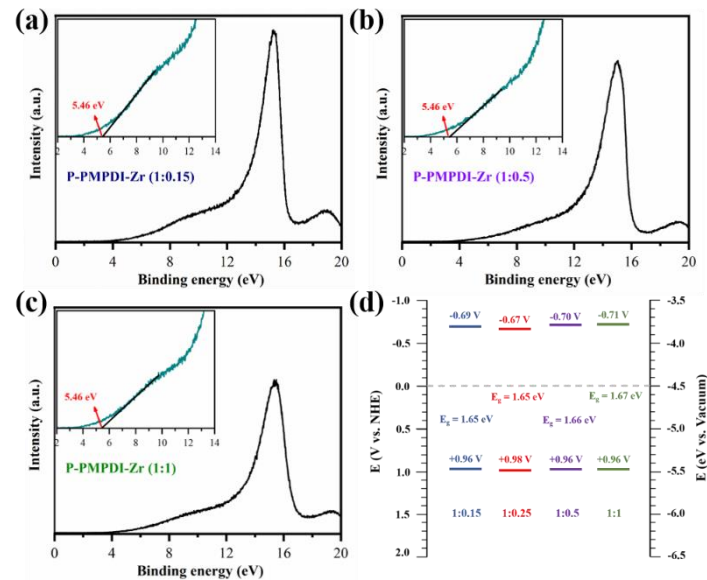


Fig. S4 (a) Ultraviolet photoelectron spectroscopy of (a) P-PMPDI-Zr (1:0.15), (b) P-PMPDI-Zr (1:0.5) and (c) P-PMPDI-Zr (1:1). Inset: linear fitting in the Fermi level region. (d) Band diagram for P-PMPDI-Zr (1:0.15), P-PMPDI-Zr (1:0.5) and P-PMPDI-Zr (1:1).

5. Light-harvesting ability and crystallinity of P-PMPDI-M

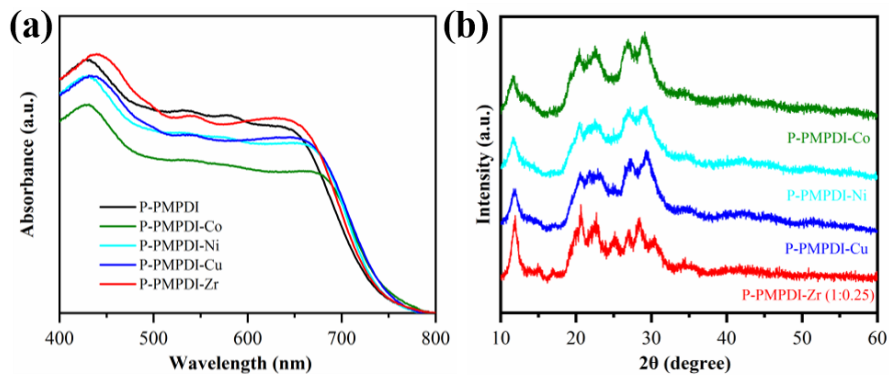


Fig. S5 (a) UV–vis DRS, (b) XRD of the **P-PMPDI**, **P-PMPDI-Co**, **P-PMPDI-Ni**, **P-PMPDI-Cu** and **P-PMPDI-Zr**. The molar ratio of P-PMPDI to M ions was 1:0.25.

6. Fourier transform infrared spectra of supramolecular

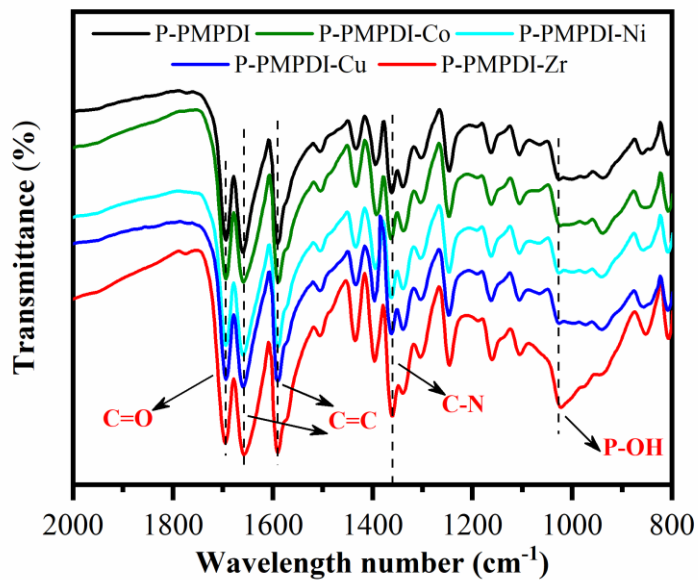


Fig. S6 Fourier transform infrared (FT-IR) spectra of **P-PMPDI-Zr**, **P-PMPDI-Co**, **P-PMPDI-Ni**, **P-PMPDI-Cu** and **P-PMPDI**

7. Density functional theory (DFT) calculations

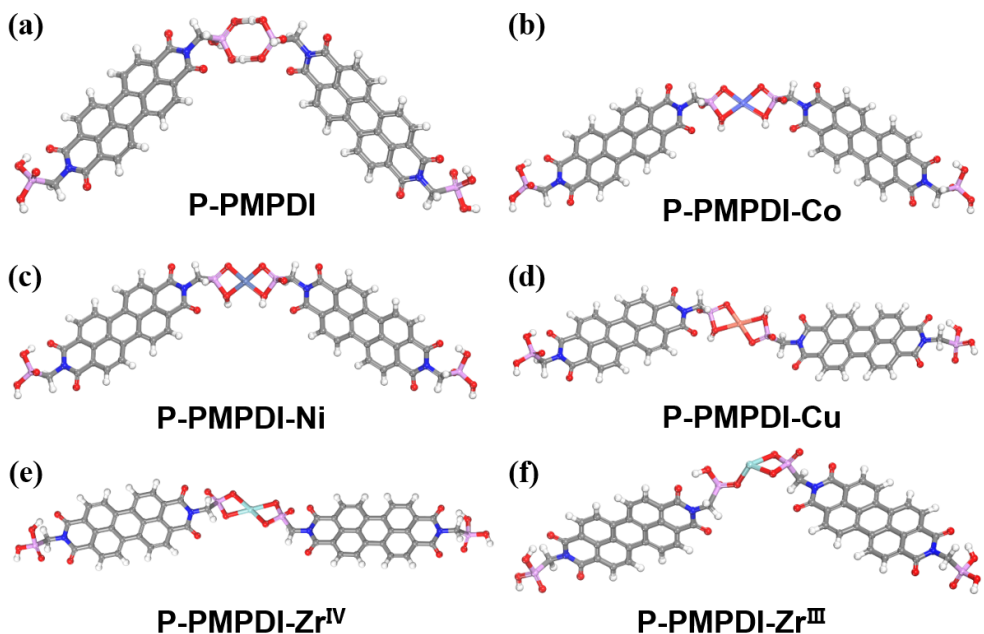


Fig. S7 Molecular model and the most stable molecular configuration of the P-PMPDI (a), P-PMPDI-Co (b), P-PMPDI-Ni (c), P-PMPDI-Cu (d), P-PMPDI-Zr^{IV} (e) and P-PMPDI-Zr^{III} (f).

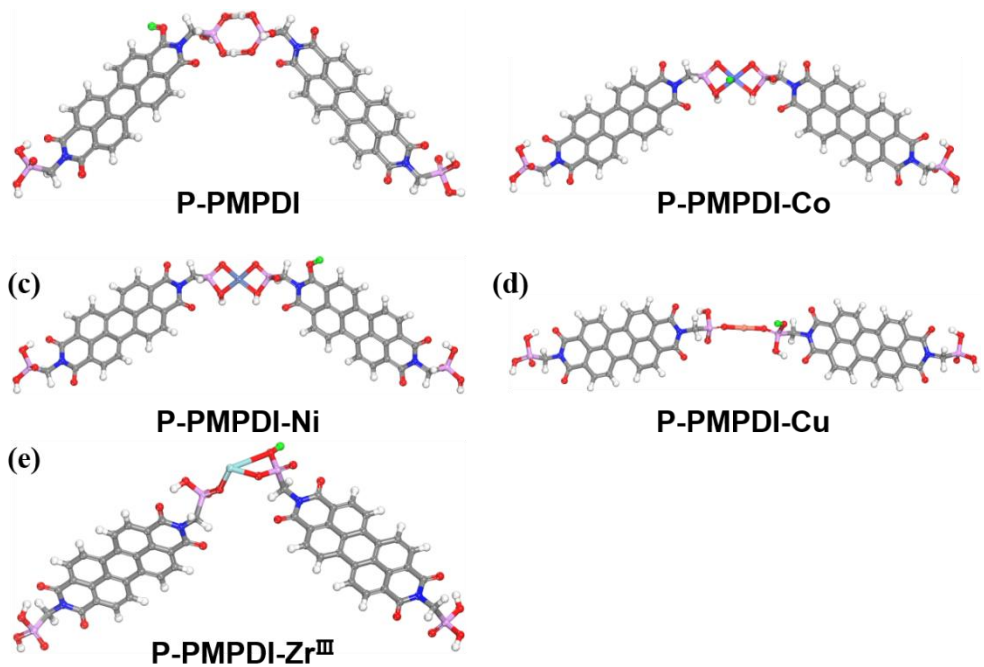


Fig. S8 DFT calculation of HER pathways. The most favorable HER intermediate of the P-PMPDI (a), P-PMPDI-Co (b), P-PMPDI-Ni (c), P-PMPDI-Cu (d) and P-PMPDI-Zr^{III} (e).

8. Calculated apparent quantum yield (AQY) at different wavelengths

$$\begin{aligned} \text{AQY } (\%) &= \frac{2 \times \text{Number of evolved } H_2 \text{ molecules}}{\text{Number of incident photons}} \times 100\% \\ &= \frac{2 \times C \times N_A}{S \times P \times t \times \frac{\lambda}{h \times c}} \times 100\% \end{aligned}$$

Where, C is the H_2 production amount (μmol) per hour; N_A is the Avogadro constant ($6.02 \times 10^{23} \text{ mol}^{-1}$); S is the irradiation area (12.56 cm^2); P is the monochromatic light intensity (W cm^{-2}) (P is detected by optical power meter); t is the light irradiation time (1 h); λ is the wavelength of the monochromatic light (nm); h is the Plank constant ($6.626 \times 10^{-34} \text{ J s}$); c is the speed of light ($3 \times 10^8 \text{ m s}^{-1}$).

Table S1. Calculated AQY at different wavelengths

Wavelength (nm)	Light intensity ($10^{-3} \text{ W cm}^{-2}$)	^a Amount of H_2 ($\mu\text{mol h}^{-1}$)	AQY (%)
420	1.96	11.01	7.07
475	2.08	18.70	10.02
500	2.46	27.04	11.64
550	2.41	27.64	11.04
630	2.12	29.61	11.70
700	2.61	4.26	1.23

a. Reaction conditions: 50 mL water, 5 g AA, 50 mg photocatalyst.

$\lambda=420 \text{ nm}$

$$\text{AQY } (\%) = \frac{2 \times 11.01 \times 10^{-6} \times 6.02 \times 10^{23}}{12.56 \times 1.96 \times 10^{-3} \times 3600 \times \frac{420 \times 10^{-9}}{6.626 \times 10^{-34} \times 3 \times 10^8}} \times 100\% = 7.07\%$$

$\lambda=475 \text{ nm}$

$$\text{AQY } (\%) = \frac{2 \times 18.70 \times 10^{-6} \times 6.02 \times 10^{23}}{12.56 \times 2.08 \times 10^{-3} \times 3600 \times \frac{475 \times 10^{-9}}{6.626 \times 10^{-34} \times 3 \times 10^8}} \times 100\% = 10.02\%$$

$\lambda=500 \text{ nm}$

$$\text{AQY } (\%) = \frac{2 \times 27.04 \times 10^{-6} \times 6.02 \times 10^{23}}{12.56 \times 2.46 \times 10^{-3} \times 3600 \times \frac{500 \times 10^{-9}}{6.626 \times 10^{-34} \times 3 \times 10^8}} \times 100\% = 11.64\%$$

$\lambda=550$ nm

$$\text{AQY (\%)} = \frac{2 \times 27.64 \times 10^{-6} \times 6.02 \times 10^{23}}{12.56 \times 2.41 \times 10^{-3} \times 3600 \times \frac{550 \times 10^{-9}}{6.626 \times 10^{-34} \times 3 \times 10^8}} \times 100\% = 11.04\%$$

$\lambda=630$ nm

$$\text{AQY (\%)} = \frac{2 \times 29.61 \times 10^{-6} \times 6.02 \times 10^{23}}{12.56 \times 2.12 \times 10^{-3} \times 3600 \times \frac{630 \times 10^{-9}}{6.626 \times 10^{-34} \times 3 \times 10^8}} \times 100\% = 11.70\%$$

$\lambda=700$ nm

$$\text{AQY (\%)} = \frac{2 \times 4.26 \times 10^{-6} \times 6.02 \times 10^{23}}{12.56 \times 2.61 \times 10^{-3} \times 3600 \times \frac{700 \times 10^{-9}}{6.626 \times 10^{-34} \times 3 \times 10^8}} \times 100\% = 1.23\%$$

9. The reported work previously

Table S2. Comparison of the photocatalytic activity among supramolecular systems.

Photocatalyst	Light Irradiation	Hydrogen Evolution Reaction (HER)	Apparent quantum yield (AQY)	Ref.
PTCDI/Pt/TiO ₂	$\lambda \geq 420$ nm	0.075 $\mu\text{mol g}^{-1} \text{h}^{-1}$	0.047% at 550 nm	⁴
PTCDI-1/Pt/g-C ₃ N ₄	$\lambda \geq 420$ nm	0.375 $\mu\text{mol g}^{-1} \text{h}^{-1}$	0.31% at 420 nm	⁵
PBI-F/PVP-Pt	$\lambda \geq 300$ nm	0.815 $\mu\text{mol g}^{-1} \text{h}^{-1}$	Not mentioned	⁶
SA-TCPP-Pt	$\lambda \geq 420$ nm	70 $\mu\text{mol g}^{-1} \text{h}^{-1}$	Not mentioned	⁷
PorFN-Pt	$\lambda \geq 420$ nm	0.2 mmol $\text{g}^{-1} \text{h}^{-1}$	Not mentioned	⁸
P-PMPDI	$\lambda \geq 400$ nm	11.7 mmol $\text{g}^{-1} \text{h}^{-1}$	2.96% at 550 nm	⁹
P-PMPDI-Zr	$\lambda \geq 400$ nm	50.48 mmol $\text{g}^{-1} \text{h}^{-1}$	11.70% at 630 nm	This work

10. References

1. B. A. Gregg and M. E. Kose, *Chem. Mater.*, 2008, **20**, 5235–5239.
2. J. T. Kirner, J. J. Stracke, B. A. Gregg and R. G. Finke, *ACS Appl. Mater. Interfaces*, 2014, **6**, 13367–13377.
3. X. J. Lv, L. X. Zha, L. Qian, X. J. Xu, Q. Bi, Z. Y. Xu, D. S. Wright and C. Zhang, *Chem. Eng. J.*, 2020, **386**, 123939.
4. S. Chen, Y. X. Li and C. Y. Wang, *RSC Adv.*, 2015, **5**, 15880–15885.
5. S. Chen, C. Wang, B. R. Bunes, Y. X. Li, C. Y. Wang and L. Zang, *Appl. Catal. A: Gen.*, 2015, **498**, 63–68.
6. M. C. Nolan, J. J. Walsh, L. L. E. Mears, E. R. Draper, M. Wallace, M. Barrow, B. Dietrich, S. M. King, A. J. Cowan and D. J. Adams, *J. Mater. Chem. A*, 2017, **5**, 7555–7563..
7. Z. J. Zhang, Y. F. Zhu, X. J. Chen, H. J. Zhang and J. Wang, *Adv. Mater.*, 2019, **31**, 1806626.
8. X. Y. Yang, Z. C. Hu, Q. W. Yin, C. Shu, X. F. Jiang, J. Zhang, X. H. Wang, J. X. Jiang, F. Huang and Y. Cao, *Adv. Funct. Mater.*, 2019, **29**, 1808156.
9. K.Y. Kong, S. C. Zhang, Y. M. Chu, Y. Hu, F. T. Yu, H. N.Ye, H. R. Ding and J. Hua, *Chem. Commun.*, 2019, **55**, 8090–8093.